15th Australasian Fluid Mechanics Conference
The University of Sydney, Sydney, Australia
13-17 December 2004

Preliminary Investigations of Vortex Rings and Jets in Cross Flow

E.R. Hassan, R.M. Kelso, G.M. Schneider and T.C.W. Lau

School of Mechanical Engineering
The University of Adelaide, S.A, 5005 AUSTRALIA

Abstract

A piston-cylinder arrangement has been designed and tested for the generation of continuous jets, fully modulated jets and individual vortex rings in cross flow. Hydrogen bubble vizualisation, Acoustic Doppler Velocimetry and dye visualisation have been implemented to test the validity of the equipment. Mean trajectories of the vortex rings and continuous jets were determined by time averaging video footage of the spatial and temporal evolution of the vortex rings and jets interacting with the cross flow. These trajectories were found to be in close agreement with trajectories quoted in the literature.

Introduction

The jet in cross-flow (JICF) is a commonly occurring flow in both industry and nature. An appealing aspect of the jet in cross flow is its enhanced mixing over the free jet. A thorough review of the topic is given by Margason [12] citing over 300 references. More recent considerations of the JICF have been Kelso, Lim and Perry [11], Smith and Mungal [14] and Cutler [3]. Jets in cross flow are primarily classified by the Jet Reynolds number, Re_j and the square root of the ratio of momentum fluxes from the jet and the cross flow. The latter term is usually referred to as the velocity ratio, R, because in the cases of same jet and cross flow fluids R is approximately equal to the ratio of the jet to cross flow velocities. Figure 1 shows the jet and cross flow velocities, the coordinate system, the jet apparatus used in the experiment and definitions of Re_j and R. The jet diameter is denoted as *d* and the kinematic viscosity of the fluid is υ. Many studies have established that the variation of the temporal velocity profile of a modulated transverse jet changes the characteristics of the resulting flow. Particular attention has been devoted to fully modulated jets. Full modulation of a jet "breaks" the jet up into discrete vortex rings [1]. Hermanson *et al.* [9], Johari *et al.* [10] and others have demonstrated that the stronger the modulation, the deeper the jet penetrates into the cross flow. A recent study on pulsed jets by Eroglu and Breidenthal [5] demonstrated that for a fixed duty cycle (ratio of time the jet is pulsed to total time between pulses), variation of pulsation frequency varied the penetration and mixing rate of the jet. Recently zero-net-mass-flux (ZNMF) jets in cross flow were investigated by Gordon *et al.* [8]. It was observed that, under certain conditions, the ZNMF JICF penetration lacked the velocity ratio dependence of the continuous JICF. Due to the differences between the steady jet and vortex ring it is necessary to define a characteristic Reynolds number for the vortex ring. Normalizing a vortex ring's circulation, Γ, by υ results in a parameter that can be considered a Reynolds number of the vortex ring [6]. This Reynolds number, Re_Γ shown in figure 1, takes into account the velocity and duration of the pulse in generating the vortex ring. Apart from low pulsing frequencies considered in Chang and Vakili [1], there have been few studies of individual vortex ring trajectories in cross flow. The current study is investigating individually pulsed vortex rings and continuous jets - two extremes of the pulsed jet duty cycle.

Experimental Arrangement

The experiments were conducted in a 500mm x 500mm working section of a closed-return water channel located at the School of Mechanical Engineering at The University of Adelaide. The frequency-controlled pump allowed steady operation at velocities below 20mm/s and up to 450mm/s. Before issuing into the cross flow, the jet fluid passed through a flow conditioning section. This section, shown in figure 1, consisted of a 9:1 conical expansion, followed by a settling section and flow straightener and a 9:1 axisymmetric contraction. See Cutler [3] for further details. The discharge pipe had a dimeter of 50mm and a length to diameter ratio, (L/d), of 4. This diameter could be further reduced using an insert consisting of a smooth contraction and a 25mm pipe of L/d=4. A circumferential dye injection port was located in the pipe wall at least 4 jet diameters upstream of the jet exit. This method of dye injection into the jet boundary layer allowed the shear layer of the jet to be uniformly marked.

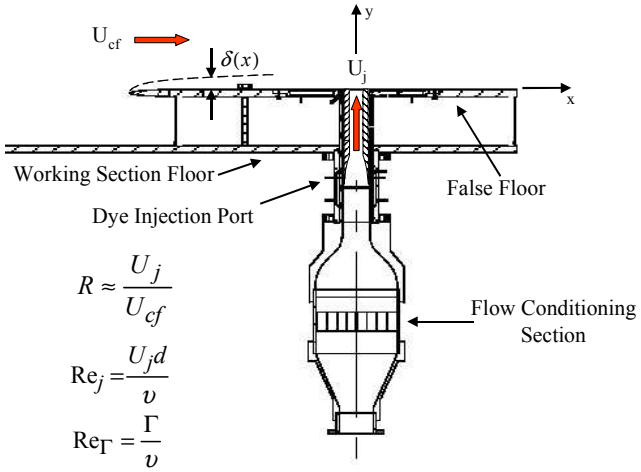

Figure 1. The jet apparatus used in the experiment showing the coordinate system. $\delta(x)$ denotes the boundary layer thickness. Reproduced and modified after Cutler and Kelso [4].

Vortex generating system

A Bellofram™ cylinder was used to generate the modulated jet flow. Fluid expelled from the cylinder travelled along a 1.5m long, 25mm diameter hose into the settling chamber and eventually issued into the working section transversely to the cross flow. A stepper motor was used in conjunction with a lead screw to advance and retract the shaft of the piston in a controlled manner. Two lead screws of pitch 2mm and 5mm were utilised. The motor controller allowed various user inputs of motor speed, drive time, pause time (and thus duty cycle) and direction. This allowed the generation of impulsively started continuous and fully modulated jets as well as individual and trains of vortex rings. Having two jet diameters of d=25mm and 50mm as well as two lead screws of pitches 2mm and 5mm provides a large range of jet velocities and Reynolds numbers. The available jet velocities ranged from 10mm/s to 650mm/s with corresponding Reynolds numbers of 500 and 16,000.

Velocity Profiles

Both the spatial and temporal jet centre-line velocities were investigated as a means of verification of the jet apparatus.

Hydrogen bubble visualisation

Hydrogen bubble visualisation (see Smith *et al* [13]) was used to observe the spatial velocity profile of the jet. The timelines were generated by a Hydrogen bubble wire mounted across the jet exit. Figure 2 shows timelines at different times after the generation of a long duration pulse. Figures 2a and 2b show the early stages of the jet and figure 2c shows the jet at a relatively well-developed stage with two successive timelines clearly visible. The images are digitally enhanced and a 5mm by 5mm grid superimposed. Hydrogen bubble visualization was conducted in this fashion over the full range of operating conditions. The results indicate a top hat velocity profile is obtained for the jet in absence of a cross flow and show symmetric roll up of the shear layer.

Acoustic Doppler Velocimetry

Three-dimensional Acoustic Doppler Velocimetry was used to measure the temporal velocity profile of the pulsed jets. The measurements were conducted using a SonTek^{TM} Acoustic Doppler Velocimeter (ADV), which had a measurement volume of 5 cubic centimetres. The measurement volume of the ADV was aligned with the centre of the jet and was located approximately one jet diameter upstream of the jet exit. The ADV supplied not only velocity components in the x, y and z directions but also correlation coefficients and signal to noise ratios for velocity signals in all three directions. A sample velocity trace of a one second pulse (τ=1 sec) with three different jet velocities is shown in figure 3. As can be seen, the profile structure, although not exactly square, is adequate of the purposes of generating fully modulated jets. The limiting property of the equipment was the rise time of the velocity from zero to the desired value. The time axis on figure 3 is normalised relative to the pulse time, τ, and the velocity axis is normalised relative to the velocity that the steady state jet would attain if continually driven at the set speed, V_{ss}.

Experiment

Dye vizualisation of jets and vortex rings in cross flow was conducted. The continuous jet was marked with neutrally buoyant dye. For all cases presented, the jet diameter is 25mm. Several minutes were allowed to elapse between each run to let the dye in the jet pipe diffuse to a relatively uniform concentration and to allow any secondary flows in the jet pipe to dissipate. The cross-flow velocity was held constant at 32mm/s for all flow cases, thereby keeping the cross-flow boundary layer thickness at the jet exit constant at δ/d=0.7. Table 1 shows flow cases considered as well as the number of the times each flow case was run.

Flow	R	U_j mm/s	Re_j	Re_Γ	No. of runs	mean at x/d=10	$U_{95\%}$ (+/-)
Jet	2	69	1,700	-	5	3.84	0.12d
Jet	4	127	3,200	-	5	5.79	0.26d
Jet	6	195	4,900	-	5	10.40	0.48d
Jet	8	252	6,300	-	5	13.48	1.10d
Ring	2	69	1,700	1,400	10	3.02	0.075d
Ring	4	127	3,200	4,800	10	8.13	0.090d
Ring	6	195	4,900	11,400	9	14.74	0.232d

Table 1. Details of the cases investigated.

Data Analysis

Video footage was digitised into a series of images and then analysed using *MATLAB*^{TM} software. Images were averaged to obtain a normalised "time exposure".

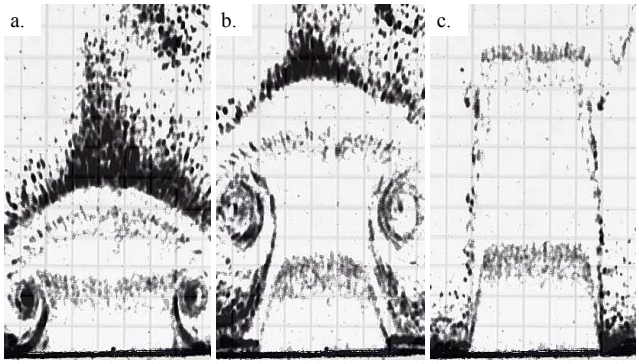

Figure 2. Time lines of an impulsively started jet. Images a, b and c correspond to times t=0.8sec, t=1.1sec and t=3.3sec respectively. The jet velocity is 123mm/s and the jet diameter is 25mm.

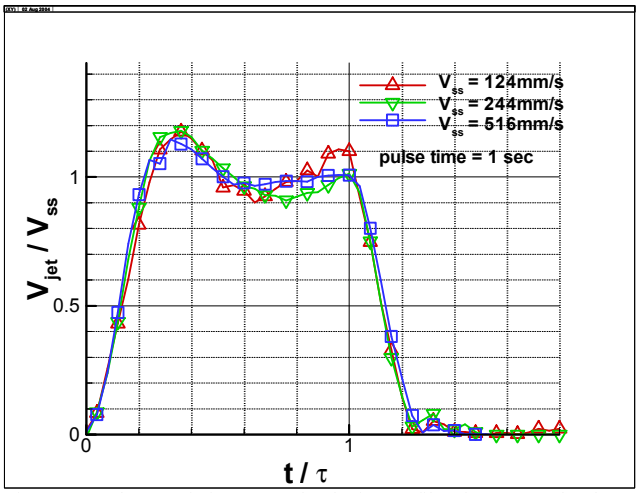

Figure 3. A characteristic temporal velocity profile of a 1 second pulse at three different jet velocities.

Mean trajectories of each flow case were obtained using a similar technique used by and Cutler [3] and Gordon [7]. The maximum concentration in vertical direction along each point on the x-axis was identified, as was maximum concentration in the horizontal direction at each point on the y-axis. This provides two approximations to the jet and vortex ring trajectories. Figure 4 and figure 5 show samples of jet and vortex ring mean image contours with the maxima in concentration in the vertical and horizontal directions overlayed. As can be seen in figure 4 the maxima in the vertical direction seem to provide a much better indication of the jet trajectory than the maxima in the horizontal direction. For the vortex ring sample, figure 5, it can be seen that both approximations to the vortex ring trajectory are consistent with the mean image. This is primarily due to the fact that the spread of the vortex ring as it travels downstream is much less than for the jet at a similar velocity ratio. The vortex ring mean image does not seem to grow more than one or two jet diameters in the range examined. Hence, the trajectories derived from maxima in the vertical direction were used exclusively to define the jet and vortex ring trajectories for this study. Table 1 shows 95% confidence intervals for the flow cases presented here based on the scatter of the maximum concentration trajectory data at x/d=10. It can be seen that the worst case scatter is approximately +/- 8%. It should be noted that there are two sources of uncertainty in the mean trajectory for each case. The first is the uncertainty based on the determination method used in estimating the trajectory. The second is the deviation of the trajectory from jet to jet or ring to ring at a fixed set of flow parameters. No attempt has been made as of yet to investigate the individual uncertainty associated with each of these two sources.

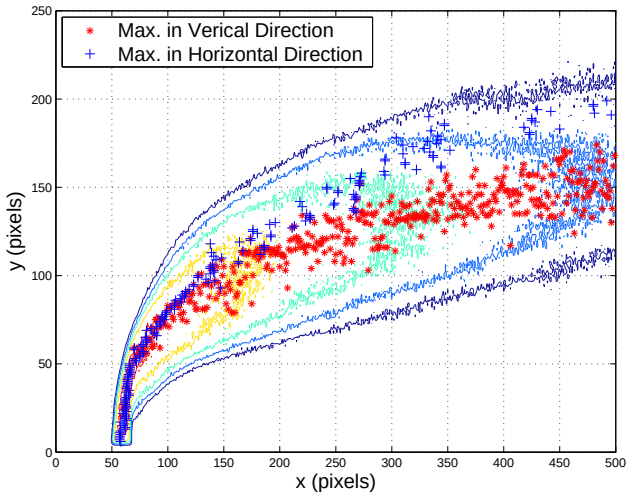

Figure 4 Trajectories based on maximum concentration in the horizontal and vertical directions overlayed on a mean jet contour plot. The velocity ratio is R=4 and jet velocity is 127mm/s. Re_j = 3,200.

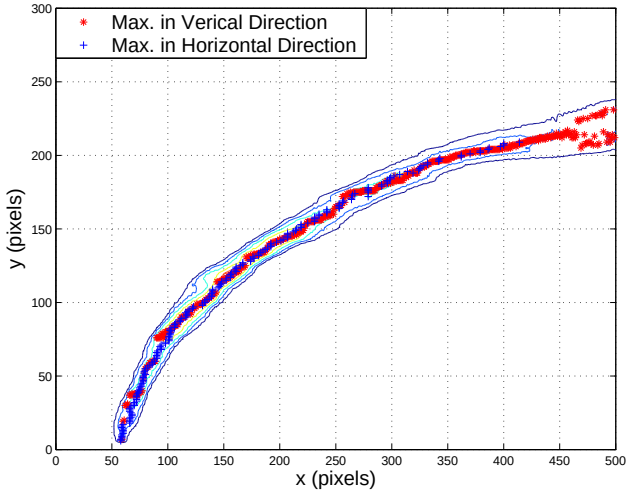

Figure 5. Trajectories based on maximum concentration in the horizontal and vertical directions overlayed on a mean vortex ring contour plot. The velocity ratio is R=4 and jet velocity is 127mm/s. Re_j = 3,200, Re_Γ = 4,800.

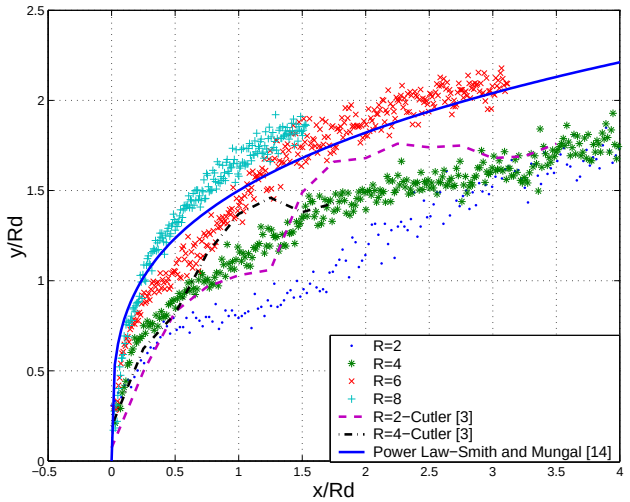

Figure 6. Rd scaling of jet trajectories based on maximum concentration in the vertical directions for R = 2, 4, 6 and 8 compared to results from Cutler [3] for R = 2(Re_j = 4,000) and R = 4 (Re_j = 8,000) and the power law obtained by Smith and Mungal [14].

Results and Discussion

Jet Trajectory

Figure 6 shows the concentration data plotted using Rd scaling, and compared with data from Cutler [3] and a power law obtained by Smith and Mungal [14]. The current data are consistent, with the trajectory height increasing with velocity ratio. The trajectories for R = 2 and 4 appear to be slightly lower than those found by Cutler [3]. The power law curve of Smith and Mungal [14] can only be used as a guide as it represents data obtained for 5<R<25.

Counter Rotating Vortex Pair

The counter-rotating vortex pair (CVP) is a large scale vortex system occurring in the jet in cross flow. This vortical structure is aligned and embedded in the jet and has been shown to originate from the jet shear layer, [2,11]. As the CVP develops and the jet bends over, the jet fluid is entrained into the CVP. Studies by Smith and Mungal [14] and Cutler [3] among others have shown that the CVP core fluid concentration is higher than the centre plane concentration. Furthermore, due to the "kidney" shape of the jet cross section and the up-wash of cross flow fluid into the underside of the jet, we expect the trajectories of the CVP to be somewhat lower than the trajectory of the jet fluid on the centreline. Figures 7 and 8 show the current data plotted with centreline and CVP trajectories from Cutler [3]. The data obtained by Cutler [3] indeed show the centreline trajectory to be higher than the CVP trajectory. The data from the present study were obtained from a side-view of the jet under uniform illumination. Thus it is expected that this method should deliver jet trajectories that lie somewhere between the CVP trajectory and the jet trajectory. Indeed, the present data show trends that match closely the data presented by Cutler [3] for a similar Re_j and in general lie closer to the CVP data. The R=2 case presented in figure 7 is also compared with centreline data from Kelso *et al* [11] and shows reasonable agreement. This provides further evidence that the new experimental equipment is adequate for the further investigation of pulsed and continuous jets in cross flow.

Vortex Ring Trajectory

Figure 9 shows comparisons between the trajectories of continuous jets and individual vortex rings. The cases for R=4 and R=6 reinforce the results obtained by Chang and Vakili [1] that the trajectories of individual vortex rings are significantly higher than those of a continuous jet for the same velocity ratio. It is interesting to note the seemingly low trajectory of the vortex ring at R=2. It was observed that, for vortex rings at R=2, the vortex ring broke down very soon after its initial formation at the jet exit. Within approximately 2 jet diameters downstream of the jet exit the vortex ring structure broke down so that the ring was apparently devoid of any vortical structure. A possible cause of this is the interaction between the low circulation vortex rings and the boundary layer fluid in the vicinity of the jet exit. It is possible that vorticity cancellation occurs between the vortex ring and the boundary layer fluid resulting in a lower vortex ring trajectory. For all of the velocity ratios considered in this study, the vortex rings left a trail of ring fluid from the jet exit to the centre of the ring. Due to the stretching of these "structures" and the subsequent thinning of the dye it is unclear weather or not they contain any vorticity. This is consistent with observations made by Chang and Vakili [1] as was the observation of a slight tilt in the higher velocity ratio rings as they moved into the cross flow.

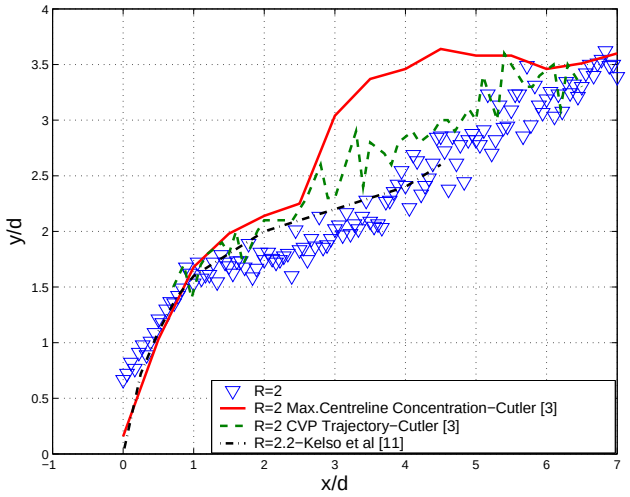

Figure 7. Jet trajectory for R=2 (Re_j = 1,700) compared to centreline and CVP trajectories from Cutler [3] for R=2 (Re_j = 4,000) and hotwire measurements from R=2.2 from Kelso *et al* [11].

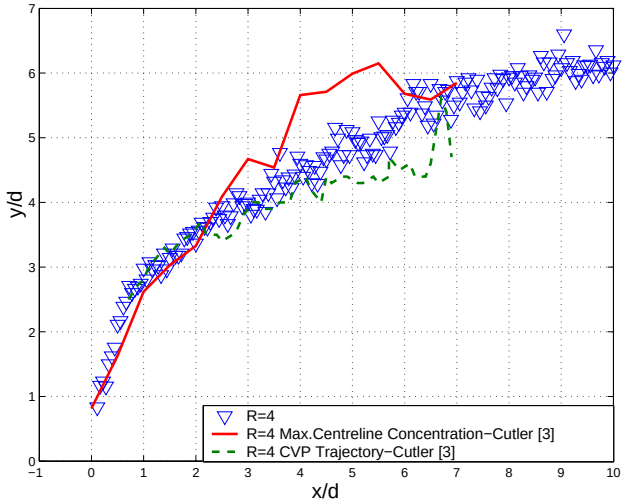

Figure 8. Jet trajectory for R=4(Re_j = 3,200) compared to centreline and CVP trajectories from Cutler [3] for R=4 (Re_j = 8,000).

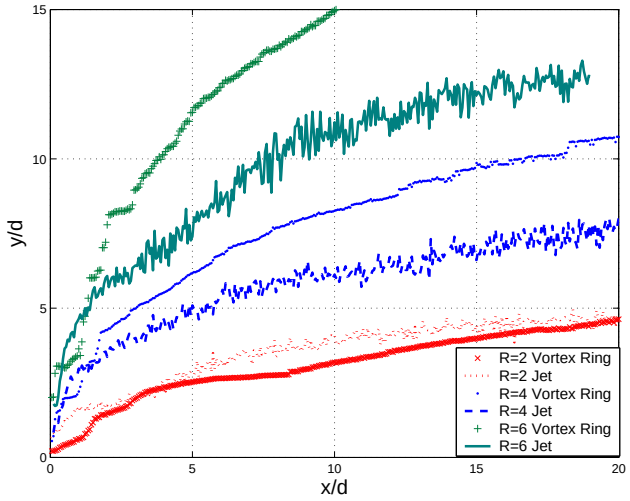

Figure 9. Jet trajectories for R=2, 4 and 6 compared to vortex ring trajectories for R=2, 4 and 6.

Conclusions

The implementation of equipment to study continuous and pulsed jets has been presented. Acoustic Doppler Velocimetry and Hydrogen bubble wire vizualisation have been used to examine the spatial and temporal velocity profile of short duration pulses and continuous jets at the jet exit. Dye vizualisation of jets and vortex rings has shown that the equipment generates flows consistent with previous work in this area. This current work has provided framework for more detailed studies of continuous jets, pulsed jets and individual vortex rings in cross flow.

Acknowledgments

Financial support in the form of a departmental scholarship from School of Mechanical Engineering at the University of Adelaide and the Frank Perry Scholarship from the University of Adelaide Postgraduate Office are acknowledged and appreciated.

References

[1] Chang, Y.K. and Vakili, A.D., Dynamics of Vortex Rings in Cross-flow. *Phys. Fluids*, **7(7),** 1995, 1583–1597.

[2] Cortelezzi, L. and Karagozian, A.R., On the Formation of the Counter-rotating Vortex Pair in Transverse Jets. *J. Fluid Mech.*, **446**, 2001, 347–373.

[3] Cutler, P.R.E, On the Structure and Mixing of a Jet in Cross-Flow. *Ph.D. Thesis.* Department of Mechanical Engineering. The University of Adelaide, 2002.

[4] Cutler, P.R.E and Kelso, R.M., On the Structural Differences Between Elevated and Flush-mounted Transverse Jets. *14th Australasian Fluid Mechanics Conference,* The University of Adelaide, 9-14 December, 2001.

[5] Eroglu, A. and Breidenthal, R.E., Structure, Penetration and Mixing of Pulsed Jets in Cross Flow. *AIAA J.*, **39(3),** 2001, 417–423.

[6] Glezer, A., The Formation of Vortex Rings. *Phys. Fluids*, **31**, 1988, 3532–3542.

[7] Gordon, M., Investigation of Zero-net-mass Flux Jets in Cross-flow using Planar-laser-induced Fluorescence, *Masters Thesis*, Department of Mechanical Engineering, Monash University, 2001.

[8] Gordon, M., Cater, J.E., and Soria, J., Investigation of the Mean Passive Scalar Field in Zero-net-mass-flux Jets in Cross-flow using Planar-laser-induced Fluorescence, *Phys. Fluids*, **16(3)**, 2004, 794–808.

[9] Hermanson, J.C, Wahba, A. and Johari, H., Duty-cycle Effects on Penetration of Fully Modulated, Turbulent Jets in Cross Flow. *AIAA J.*, **36(10)**, 1998, 1935–1937.

[10] Johari, H., Pacheco-Tougas, M., and Hermanson, J.C., Penetration and Mixing of Fully Modulated Turbulent Jets in Cross-flow. *AIAA J.*, **37(7),** 1999, 842–850.

[11] Kelso, R.M., Lim, T.T. and Perry, A.E, An Experimental Study of Round Jets in Cross-flow, *J. Fluid Mech.*, **306**, 1996, 111–144.

[12] Margason, R.J., Fifty Years of Jet in Cross Flow Research. *Computational and Experimental Assessment of Jets in Cross Flow*, AGRAD, 1993.

[13] Smith, C.R., Seal, C.V., Praisner, T.J. and Sabatyino, D.R., Hydrogen Bubble Vizualisation in *Flow Vizualisation*, editors T.T. Lim and A.J. Smits, Imperial College Press, 2000, 27-42.

[14]Smith, S.H. and Mungal, M.G., Mixing, Structure and Scaling of the Jet in Cross-Flow. *J. Fluid Mech.*, **357**, 1998, 83–122.